Interferometric Phase Unwrapping for W-Band GBSAR: Experiments on Simulated Signal

Mina Mohammadi [1], Jalal Amini[1,*] , Benyamin Hosseiny [2]
[1] School of Surveying and Geospatial Engineering, College of Engineering, University of Tehran, Tehran, Iran - (minamohammadi, jamini)@ut.ac.ir
[2] School of Computer Science, University of Bristol, Bristol, UK - ben.hosseiny@bristol.ac.uk

Keywords: phase unwrapping, displacement monitoring, Radar, Goldstein's Branch-Cut, quality-guided.

Abstract

Displacement monitoring of structures and the Earth's surface have always been of great importance, aiming to minimize human casualties and financial losses. One of the prominent methods is radar interferometry using various types of radar sensors. Specifically, GBSAR (Ground-Based Synthetic Aperture Radar) sensors have gained more attention for this purpose. Recent GBSAR developments tend to using shorter wavelengths for displacement monitoring, such as mmWave W band. However, decreasing the wavelength increases the chance of phase wrapping and unwrapping error. This paper analyses the performance of prominent phase unwrapping techniques on a W-band GBSAR sensor. Various simulated scenarios have been conducted, and subsequently, to solve the unwrapping problem, temporal and spatial techniques, including Goldstein's Branch-Cut and quality-guided algorithms have been investigated. The results show better performance of Goldstein's Branch-Cut algorithm compared to the quality-guided method, with RMSE values for displacement extraction of 0.122 and 0.154 mm, respectively. Moreover, Goldstein's Branch-Cut algorithm also demonstrated a faster processing speed.

1. Introduction

Synthetic Aperture Radar Interferometry (InSAR) is a well-established and powerful remote sensing technique that enables the highly accurate measurement of key geophysical parameters. These include surface topography, ground deformation, land subsidence, and glacier movements (Moreira et al., 2013).

Radar interferometry is based on comparing the phase of two or more complex SAR (Synthetic Aperture Radar) images of a specific area, acquired from slightly different positions or at different times. Since the phase of each pixel in SAR images contains information about the range (distance) to the target, it is possible to detect and measure extremely subtle changes in the propagation path of the radar waves with an accuracy of a fraction of the radar wavelength, on the order of centimeters or even millimeters. This characteristic, combined with SAR's ability to capture images under all weather conditions and during both day and night, has made radar interferometry a powerful tool for airborne, spaceborne, and ground-based remote sensing.

Over the past two decades, ground-based radar sensors have gained increasing attention among researchers due to their advantages, such as high accuracy, wide coverage with a high spatiotemporal resolution , low construction cost, quick deployment, and the capability to monitor deformation phenomena with a wide range of rates—from a few millimeters per year to over a meter per hour (Long et al., 2018; Zhu et al., 2021). The system's high sensitivity to small deformations, its long-range measurement capability (spanning several kilometers), and its imaging capability, which allows for a large number of simultaneous measurements, are key features that make the GBSAR (Ground-Based Synthetic Aperture Radar) system a valuable complement to other deformation measurement techniques (Monserrat et al., 2014).

The interferometric phase, which is considered the primary observable in a GBSAR system, is defined by Equation (1), assuming that GBSAR acquisitions are typically performed with a zero-baseline configuration and therefore do not include topographic phase contributions.

$$\Delta\varphi_{21} = \varphi_2 - \varphi_1 = \varphi_{defo} + \varphi_{atm} + \varphi_{noise} + 2.K.\pi \quad , \quad (1)$$

Where φ_{defo} refers to the phase component associated with displacement, φ_{atm} represents the atmospheric phase contribution caused by atmospheric effects at the time of image acquisition, and φ_{noise} denotes the phase component related to noise sources such as instrumental noise (Monserrat et al., 2014).

Phase unwrapping is one of the key and most challenging steps in phase extraction. Achieving an unwrapped phase without significant loss of signal resolution is particularly important in many applications, such as displacement monitoring. Phase unwrapping is the process of converting a wrapped phase, confined within the modulo 2π range of [−π,π], into a continuous phase signal with a wider dynamic range than [−π,π]. The relationship between the wrapped phase and the unwrapped phase is given in Equation (2):

$$\bar{\emptyset}(x,y) = \emptyset(x,y) + 2k\pi \quad , \quad (2)$$

In this equation, $\bar{\emptyset}(x,y)$ represents the unwrapped phase, while $\emptyset(x,y)$ denotes the wrapped phase (Estrada et al., 2012). Numerous phase unwrapping methods have been developed, which can generally be categorized into one-dimensional (temporal) and two-dimensional (spatial) techniques. All existing phase unwrapping approaches are fundamentally based

* Corresponding author

on the assumption that the discrete derivatives of the unwrapped phase, i.e., the differences between neighboring pixels, can be accurately determined, provided these differences remain below a certain threshold (typically π) (Costantini, 2002).

In 1988, Goldstein and colleagues introduced the well-known Goldstein algorithm for phase unwrapping. In addition to addressing the challenge of radar phase measurements being wrapped in modulo 2π, they also recognized noise and geometric effects, such as layover, as contributors to local phase measurement errors. By proposing a method based on residue computation, they successfully derived a digital elevation model (DEM) from the unwrapped phase data (Goldstein et al., 1988).

In (Davidson and Bamler, 2002), a method for two-dimensional phase unwrapping in SAR interferometry was proposed, involving both coarse and fine phase estimation. Using an adaptive multi-resolution technique, interferometric fringe frequencies are estimated, and the coarse phase is reconstructed using a weighted least squares method. This coarse phase is then applied in adaptive slope filtering to reduce phase variations, and finally, the fine phase is reconstructed using weights obtained through morphological operations. The method was validated on both simulated and real datasets. Another study introduced a novel 2D phase unwrapping algorithm that segments the image into multiple regions and unwraps them progressively using a least squares approach. The method, implemented based on the finite element method (FEM), was shown to reduce errors and outperform previous techniques on both simulated and real SAR data (Fornaro and Sansosti, 2002). The article (Just et al., 1995) reviews and compares two major phase unwrapping approaches: branch-and-cut and least squares (LS) techniques in SAR interferometry. The authors analyze how each method handles phase residues caused by noise or undersampling. While the branch-and-cut method directly addresses these residues, the LS approach's handling of them is not as clearly defined. The paper clarifies this issue and establishes a connection between LS approaches and integral-based methods.

In (Estrada et al., 2012), the performance of the Recursive Phase Unwrapping (RPU) system was compared with two other methods: the well-known Goldstein branch-cut algorithm and the Regularized Phase Tracker (RPT). Unlike branch-cut methods, RPU does not require marking phase inconsistencies. The results demonstrated that RPU is an innovative, fast, and robust technique for 2D phase unwrapping.

Another study compared various quality-guided phase unwrapping techniques to determine the most suitable quality map and guiding strategy. Results showed that transform-based methods performed best under noisy conditions, but were insufficient in the presence of discontinuities. Among the guiding strategies, the classical approach provided the highest accuracy, while the chain-stack strategy offered superior speed (Zhao et al., 2011).

In (Zhang et al., 2019), the performance of three 2D phase unwrapping algorithms, Branch-Cut (BC), Minimum Discontinuity (MD), and Fast Phase Unwrapping (FPU), was evaluated under noisy conditions. Results indicated that while MD is highly robust to noise, it is slower than the other two methods. To address this, two hybrid algorithms were developed by combining MD with BC and FPU, respectively. These hybrid algorithms combine the high speed of BC and FPU with the noise resilience of MD. Simulation and real-data experiments confirmed the improved accuracy and speed of these hybrid approaches.

This paper investigates two spatial phase unwrapping algorithms; Goldstein's method and the quality-guided approach combined with temporal phase unwrapping applied to a simulated phase time series. The main objective of this study is to evaluate the performance of the proposed simulated method for potential application to mmWave W band GBSAR time-series data.

2. Method

Given the importance of phase unwrapping accuracy in the precise estimation of displacement, this study evaluates a method for three-dimensional phase unwrapping of a simulated phase in the frequency band of a GBSAR sensor within a controlled simulation environment. The GBSAR system under consideration utilizes the AWR1642 radar module, operating in the W-band frequency range (76–81 GHz) with an approximate wavelength of 4 mm. This sensor supports signal bandwidths up to 4 GHz, enabling a range resolution of approximately 4 cm. Some of the sensor characteristics are presented in the table 1 (Hosseiny et al., 2023, 2024).

Parameters of Radar Sensor	Experiments
Radars sensor model	TI-AWR1642BOOST
Signal type	Linear FMCW
Carrier frequency	76-81 GHz
Signal bandwidth	<4 GHz
Vertical rail length	<0.9 m

Table 1. GBSAR Sensor Characteristics

The overall methodology is illustrated in Figure 1: a phase is initially generated over an image with dimensions of 512 × 256 pixels, and a predefined displacement is applied for each epoch. Subsequently, speckle and Gaussian noise with a variance of 0.1 rad are added to the simulated phase.

Since the simulation is carried out in three dimensions, the 3D phase unwrapping problem is decomposed into a 1D temporal and a 2D spatial phase unwrapping process. This decomposition simplifies the problem and makes it more tractable. Finally, to assess the performance of the phase unwrapping algorithm in displacement estimation, the retrieved displacement is evaluated using the two selected unwrapping algorithms.

This contribution has been peer-reviewed. The double-blind peer-review was conducted on the basis of the full paper.
https://doi.org/10.5194/isprs-annals-X-4-W8-2025-525-2026 | © Author(s) 2026. CC BY 4.0 License.

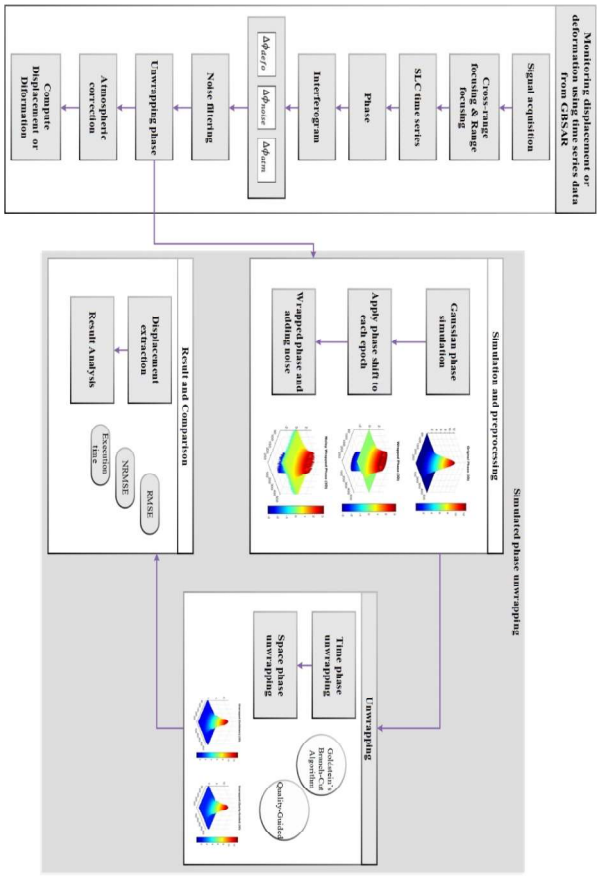

Figure 1. Flowchart of the proposed method

2.1 Temporal Phase Unwrapping

The fundamental principle of the one-dimensional phase unwrapping method, originally proposed by Itoh (Itoh, 1982), is as follows: For a sequence of m discrete wrapped phase measurements $[\phi_1^w, \phi_2^w, \dots, \phi_n^w]$, the unwrapped interferometric phase $\varphi_{1,k} = \phi_1 - \phi_k$ can be calculated from the interferograms obtained at different time instances using single-look radar images, as shown in Equation (3):

$$\begin{aligned}\varphi_{1,k} = \phi_1^w - \phi_2^w - 2\pi n_{12} + \phi_2^w - \phi_3^w \\ - 2\pi n_{23} + \cdots + \phi_{k-1}^w - \phi_k^w \\ - 2\pi n_{k-1,k} \\ = \phi_1^w - \phi_k^w \\ - 2\pi(n_{12} + n_{23} + \cdots \\ + n_{k-1,k}), (k = 1,2,\dots,m)\end{aligned} \quad , \qquad (3)$$

From the above equation, it is evident that as long as the phase ambiguity number $n_{k-1,k}$ between two single-look images is zero, meaning temporal continuity is preserved, the unwrapped interferometric phase at any given time can be correctly φ_k determined.

In practice, during radar signal acquisition, as long as the radar signal sampling rate is sufficiently high to detect phase cycle slips, it can be guaranteed that $n_{k-1,k} = 0$, ensuring accurate unwrapping results.

In other words, if the sampling rate satisfies the Nyquist criterion, the phase jumps become identifiable, and the interferometric phase between consecutive images can be calculated as shown in Equation (4) (Xiang et al., 2022):

$$\varphi_{k-1,k} = \phi_{k-1}^w - \phi_k^w - 2\pi n_{k-1,k} = \phi_{k-1}^w - \phi_k^w \quad , \qquad (4)$$

2.2 Space Phase Unwrapping

2.2.1 Goldstein's Branch-Cut Algorithm: The Goldstein Branch-Cut algorithm is one of the classic and widely used methods for two-dimensional phase unwrapping. The algorithm identifies phase discontinuities and creates barriers called branch cuts between them to define consistent paths for phase reconstruction.

Initially, discontinuity points are detected using closed 2×2 loops in the wrapped phase map. The discontinuity value R(i,j) at coordinates (i,j) is calculated by summing the phase gradients in a clockwise direction ,as shown in Equation (5).

$$\begin{aligned}R(i,j) = \sum_{m=1}^{4} \Delta_m \\ = [\psi(i,j+1) - \psi(i,j)] \\ + [\psi(i+1,j+1) - \psi(i,j \\ + 1)] + [\psi(i+1,j) - \psi(i \\ + 1,j+1)] + [\psi(i,j) \\ - \psi(i+1,j)]\end{aligned} \quad , \qquad (5)$$

Where Δm represents the gradient of the 2×2 closed loop of the wrapped phase with $m \in [1,4]$, and ψ(i,j) represents the wrapped phase. If the sum of these gradients is zero, the corresponding pixel is not considered a residue; otherwise, it is labeled as a residue, either positive or negative discontinuity.

A residue is positive when NINT [R(i,j)/(2π)]=1 (Wang and Yang, 2019), and negative when NINT [R(i,j)/(2π)]=-1. Next, a residue is randomly selected and set as the search center. A 3×3 neighborhood around it is examined to locate other residues. If another residue is found, it is connected to the original residue using a branch cut.

- If the found residue has opposite polarity, the original residue is neutralized and the branch cut terminates.
- If the found residue has the same polarity, the search center moves to the new residue, and the search continues.

Ultimately, the unwrapping path must avoid crossing branch cuts, and pixels lying on branch cuts are unwrapped using their neighboring pixels.

A correct implementation of the algorithm must also address two important considerations:

1. Every time a residue is encountered during the search, it must be connected to the current residue via a branch cut—even if it has already been connected via another branch cut.
2. If the search encounters a pixel at the image boundary, a branch cut should be drawn from the residue to the edge of the image to maintain residue balance.

This algorithm is very fast, requires minimal memory, and generally reconstructs phase data correctly. However, its main drawback is that it does not utilize additional information from

the phase data, such as quality maps or masks, to guide the placement of branch cuts (Pritt, 1997).

2.2.2 Quality-Guided Phase Unwrapping: The basic assumption of the quality-guided method is that high-quality pixels are less likely to cause phase unwrapping errors (Ghiglia, 1998). These methods always try to build the integration path in such a way that it first passes through pixels with the highest quality (based on the quality map). Therefore, the performance of quality-guided methods is highly dependent on the quality map used (Yu et al., 2019).

In the quality-guided phase unwrapping algorithm, a quality map is first computed for the 2D signal using a quality metric applied to each pixel. Then, each horizontal and vertical edge in the image is assigned a quality value based on the quality of the two adjacent pixels. Next, all these edges are sorted in descending order based on their quality and placed in a queue. At this stage, each pixel is assigned to a separate group. Then, the algorithm sequentially examines the edges in the queue; if the two pixels of an edge belong to the same group, that edge is ignored. If they are in different groups, using the unwrapping operator, the appropriate multiple of 2π is calculated to unwrap the second pixel relative to the first, and this value is added to all pixels of the second group. The two groups are then merged. This process continues until the end of the queue (Arevalillo-Herráez et al., 2016).

3. Results

The performance of the experiments was evaluated both qualitatively and quantitatively on simulated GBSAR data. Figure 2 shows the original phase and the results of phase wrapping, noise addition, and three-dimensional phase unwrapping using two algorithms: Goldstein and quality-guided. Visually, the phase unwrapping results from both algorithms show little difference, and both perform well in unwrapping the phase.

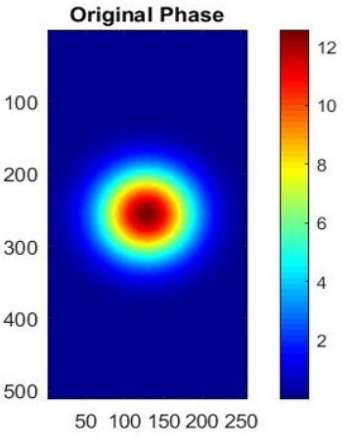

(a)

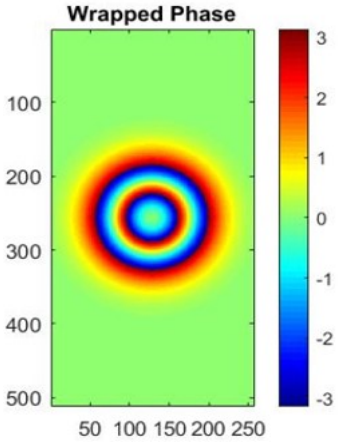

(b)

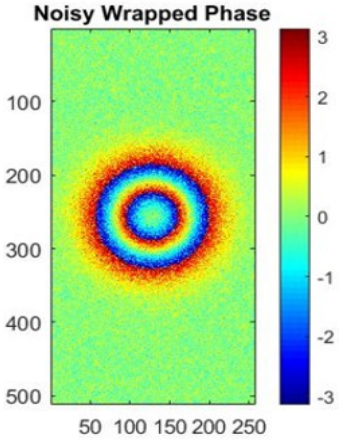

(c)

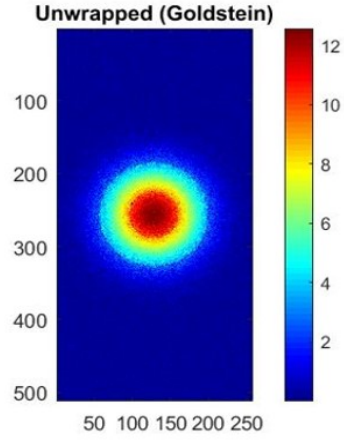

(d)

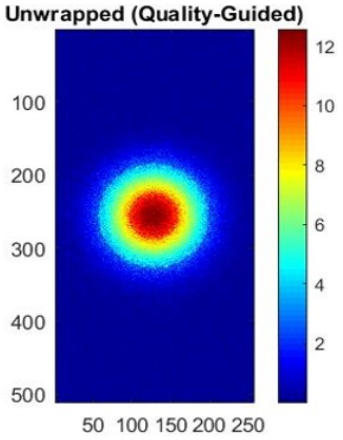

(e)

Figure 2. Result of phase unwrapping: (a) Original Phase, (b) Wrapped Phase, (c) Noisy wrapped phase, (d)Unwrapped phase based on (Temporal + Goldstein's Brunch-cut), (e) Unwrapped phase based on (Temporal + Quality-Guided)

To quantitatively assess the phase unwrapping algorithms, a cross-sectional profile from one row of the phase image at the final epoch is presented in Figure 3. The horizontal axis represents the column indices, while the vertical axis shows the phase values. This plot includes four curves, each representing a stage of phase processing.

The blue curve depicts the original phase measured before any wrapping or unwrapping. The black curve shows the wrapped phase confined within the interval [−π, π], which exhibits discontinuities due to the nature of phase wrapping. The yellow curve corresponds to the noisy wrapped phase, and the red curve represents the unwrapped phase obtained using the proposed phase unwrapping algorithm.

As seen in the red curve, the unwrapping algorithm successfully corrects the discontinuities present in the wrapped phase and produces a continuous signal that closely matches the original phase. This demonstrates the algorithm's effectiveness in reconstructing the initial phase signal. Minor fluctuations observed in the red curve correspond to residual noise in the unwrapped phase.

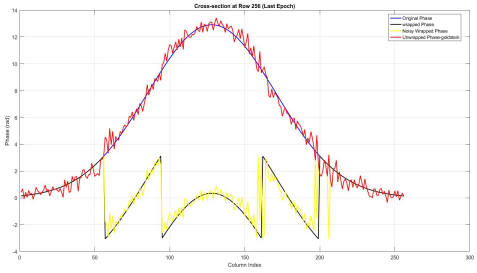

(a)

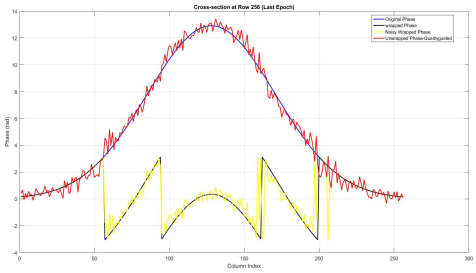

(b)

Figure 3. Cross-sectional profile from the middle row of the phase image at the final epoch: (a) Goldstein's Branch-Cut algorithm, (b) Quality-guided algorithm

Furthermore, the proposed method's performance in displacement estimation was also examined. Figure 4 illustrates the cumulative average displacement over 10 epochs, showing that the displacement estimated using the Temporal + Goldstein's Branch-Cut phase unwrapping algorithm is closer to the true displacement.

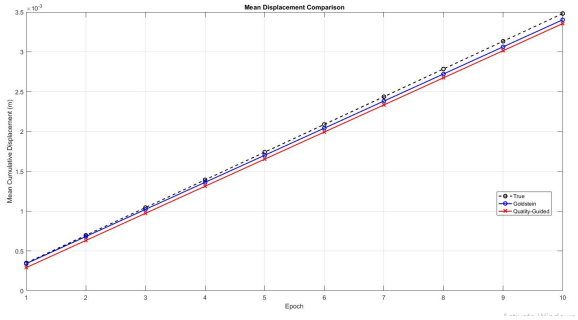

Figure 4. Comparison of Mean Cumulative Displacement

Table 2 compares the accuracy and processing time of the two three-dimensional phase unwrapping algorithms in displacement extraction. According to the results, the Temporal + Goldstein's Branch-Cut and Temporal + Quality-guided methods achieved accuracies of 0.122 and 0.154 mm, respectively. In terms of processing speed, the Temporal + Goldstein's Branch-Cut algorithm is faster than the Temporal + Quality-guided approach.

Method	RMSE (mm)	NRMSE	Processing Time (s)
Temporal + Goldstein's Branch-Cut	0. 122	0.030471	94.835
Temporal + Quality guided	0. 154	0.038585	2511.353

Table 2. Evaluation results of simulated experiments

The results obtained in this study have practical implications for deformation monitoring using GBSAR sensors. The superior performance of the Goldstein's Branch-Cut algorithm in terms

of both accuracy and processing speed indicates that it can be effectively applied to phase unwrapping in displacement monitoring scenarios, such as landslide observation, dam stability assessment, and structural health monitoring. Therefore, the proposed combined spatiotemporal phase unwrapping framework can significantly enhance the reliability of deformation measurements in W-band GBSAR sensor.

4. Conclusion

From the past until now, the issue of ground and structural displacement, has been of great importance due to its potential to cause significant human and financial losses. Radar sensors, particularly GBSAR sensors, are among the essential tools for displacement monitoring, relying on the principle of radar interferometry to extract displacement and deformation measurements. However, due to radar limitations, the interferometric phase is always confined within the interval $[-\pi,\pi]$. In cases of rapid displacement, the phase difference may exceed this defined interval, causing ambiguity in the data. Therefore, phase unwrapping is essential to achieve accurate results.

This paper examined a phase unwrapping method for time-series data aimed at simulating GBSAR data. In this approach, a phase within the frequency band of the GBSAR sensor was simulated as a time series. For phase unwrapping, a one-dimensional temporal algorithm was first applied to the time-series phase, followed by the separate application of two spatial algorithms: Goldstein's Branch-Cut and Quality-Guided.

The results indicated that the method, when using Goldstein's Branch-Cut algorithm for spatial phase unwrapping, performed better, with an RMSE approximately 0.032 mm lower than that of the Quality-Guided method. Additionally, the processing speeds of the algorithms were evaluated, showing that Goldstein's Branch-Cut required approximately 94.8 seconds, while the Quality-Guided algorithm took around 2511.4 seconds.

Although this study is based on simulated GBSAR data, the simulation parameters were selected to closely resemble the real operating conditions of W-band GBSAR sensor. Future work will include validation using actual field measurements to further verify the algorithm performance under real-world atmospheric and geometric conditions. Additionally, more complex deformation patterns and noise distributions will be simulated to extend the current analysis.

References

Arevalillo-Herráez, M., Villatoro, F. R., Gdeisat, M. A., 2016: A robust and simple measure for quality-guided 2D phase unwrapping algorithms, IEEE Trans. Image Process.,25,2601-2609.doi.org/10.1109/TIP.2016.2551370.

Costantini, M., 2002: A novel phase unwrapping method based on network programming, IEEE Trans. Geosci. Remote Sens., 36, 813-821. doi.org/10.1109/36.673674

Davidson, G. W., Bamler, R., 2002: Multiresolution phase unwrapping for SAR interferometry, IEEE Trans.Geosci .Remote Sens., 37, 163-174. doi.org/10.1109/36.739150.

Estrada, J. C., Servin, M., Vargas, J., 2012: 2D simultaneous phase unwrapping and filtering: A review and comparison. Opt. Lasers Eng., 50, 1026-1029. doi.org/10.1016/j.optlaseng.2012.01.008.

Fornaro, G., Sansosti, E., 2002: A two-dimensional region growing least squares phase unwrapping algorithm for interferometric SAR processing, IEEE Trans. Geosci. Remote Sens ,37, 2215-2226. doi.org/10.1109/36.789618.

Ghiglia, D. C., 1998: Two-dimentional phase unwrapping: Theory, Algorithms, and Software.

Goldstein, R. M., Zebker, H. A., Werner, C. L., 1988: Satellite radar interferometry: Two-dimensional phase unwrapping, Radio Sci, 23, 713-720. doi.org/10.1029/RS023i004p00713.

Hosseiny, B., Amini, J., and Aghababaei, H., 2023: Structural displacement monitoring using ground-based synthetic aperture radar, Int. J. Appl. Earth Obs. Geoinf., 116, 103144. doi.org/10.1016/j.jag.2022.103144.

Hosseiny, B., Amini, J., and Aghababaei, H., 2024: Spectral estimation model for linear displacement and vibration monitoring with GBSAR system, Mech. Syst. Signal Process., 208, 110916. doi.org/10.1016/j.ymssp.2023.110916.

Itoh, K., 1982: Analysis of the phase unwrapping algorithm, Appl. Opt., 21, 2470-2470. doi.org/10.1364/AO.21.002470.

Just, D., Adam, N., Schwabisch, M., and Bamler, R., 1995: Comparison of phase unwrapping algorithms for SAR interferograms, International Geoscience and Remote Sensing Symposium, IGARSS'95. Quantitative Remote Sens. Sci. Appl., 767-769. doi.org/10.1109/IGARSS.1995.520580.

Long, S., Tong, A., Yuan, Y., Li, Z., Wu, W., Zhu, C., 2018: New approaches to processing ground-based SAR (GBSAR) data for deformation monitoring, Remote Sens., 10, 1936. doi.org/10.3390/rs10121936

Monserrat, O., Crosetto, M., and Luzi, G., 2014: A review of ground-based SAR interferometry for deformation measurement, ISPRS J. Photogramm. Remote Sens.,93,40-48. doi.org/10.1016/j.isprsjprs.2014.04.001.

Moreira, A., Prats-Iraola, P., Younis, M., Krieger, G., Hajnsek, I., and Papathanassiou, K. P., 2013: A tutorial on synthetic aperture radar, IEEE Geosci. Remote Sens. Mag., 1, 6-43. doi.org/10.1109/MGRS.2013.2248301.

Pritt, M. D., 1997: Comparison of path-following and least-squares phase unwrapping algorithms, IGARSS'97. IEEE Int. Geosci., Remote Sens. Symp. Proc., 872-874. doi.org/10.1109/IGARSS.1997.615283.

Wang, J., Yang, Y., 2019: Branch-cut algorithm with fast search ability for the shortest branch-cuts based on modified GA, J. Mod. Opt., 66, 473-485. doi.org/10.1080/09500340.2018.1548663.

Xiang, X., Chen, C., Wang, H., Xing, C., Chen, J., Zhu, H., 2022: An improved method of GB-SAR phase unwrapping for landslide monitoring, Front. Earth Sci., 10, 973320. doi.org/10.3389/feart.2022.973320.

Yu, H., Lan, Y., Yuan, Z., Xu, J., and Lee, H., 2019: Phase unwrapping in InSAR: A review, IEEE Geosci. Remote Sens. Mag., 7, 40-58. doi.org/10.1109/MGRS.2018.2873644.

Zhang, Q., Han, Y., and Wu, Y., 2019: Comparison and combination of three spatial phase unwrapping algorithms, Opt. Rev., 26, 380-390. doi.org/10.1007/s10043-019-00513-7.

Zhao, M., Huang, L., Zhang, Q., Su, X., Asundi, A., and Kemao, Q., 2011: Quality-guided phase unwrapping technique: comparison of quality maps and guiding strategies, Appl. Opt., 50, 6214-6224. doi.org/10.1364/AO.50.006214.

Zhu, Y., Xu, B., Li, Z., Hou, J., Wang, Q., 2021. Monitoring bridge vibrations based on GBSAR and validation by high-rate GPS measurements, IEEE J. Sel. Top. Appl. Earth Obs. Remote Sens., 14, 5572-5580.
doi.org/10.1109/JSTARS.2021.3083494.